Enhancement of YBCO Thin Film Thermal Stability under 1 ATM Oxygen Pressure by Intermediate Cu_2O Nanolayer

L. Cheng,[†] X. Wang,[†] X. Yao,*[,†,‡] W. Wan,[§] F. H. Li,[§] J. Xiong,[||] B. W. Tao,[||] and M. Jirsa[⊥]

Department of Physics, Key Laboratory of Artificial Structures and Quantum Control, Ministry of Education, State Key Laboratory for Metal Matrix Composites, Shanghai Jiao Tong University, 800 Dongchuan Road, Shanghai 200240, P. R. China, Beijing National Laboratory for Condensed Matter Physics, Institute of Physics, Chinese Academy of Sciences, P.O. Box 603, Beijing 100080, People's Republic of China, State Key Lab of Electronic Thin Films and Integrated Devices, University of Electronic Science and Technology of China, 610054 Chengdu, People's Republic of China, and Institute of Physics ASCR, Na Slovance 2, v.v.i., CZ-182 21 Praha 8, Czech Republic

Received: December 14, 2009; Revised Manuscript Received: April 8, 2010

The melting process of $YBa_2Cu_3O_x$ (YBCO or Y123) films under an oxygen atmosphere was observed in situ by means of high-temperature optical microscopy. The films were classified by pole figure measurement as *c*-axis oriented, with two different in-plane orientations (denoted as 0 and 45°). In the 45°-oriented films, electron diffraction and high-resolution transmission electron microscopy (HRTEM) detected an intermediate Cu_2O nanolayer in the vicinity of the interface. The melting mode and the thermal stability of the YBCO thin films with different in-plane orientations were greatly influenced by oxygen partial pressure. Notably, the thermal stability of the 45°-oriented YBCO films dramatically grew with increasing oxygen partial pressure. We attributed this effect to a change in the intermediate Cu_2O nanolayer thermal stability. We conclude and suggest that the thermal stability of YBCO films can be significantly enhanced by inserting a Cu_2O buffer nanolayer.

Introduction

Superconductors have attracted considerable attention for nearly 100 years. In the early times, after the discovery of superconductivity in pure Hg below 4.23 K (in 1911[1]), the search for new superconductors was mainly limited to pure metallic elements (type I superconductors), and it took rather long time until superconductivity was found in alloys, some of which appeared to be type II superconductors applicable in practice. A big excitation in 1986 caused the rise of critical temperature record to 30 K, obtained by substituting Ba in La−Cu−O.[2] After the discovery of $YBa_2Cu_3O_7$ (YBCO or Y-123) in 1987,[3] an extensive effort has been focused on research and applications of high-T_c wires, tapes, thin films, as well as bulk materials. YBCO thin films as 2D oxide materials have attracted considerable interest as principal parts in the technology of coated conductors and electronic devices.

Recently, superheating effect was discovered in YBCO/MgO thin-film-seeded $NdBa_2Cu_3O_x$ (NdBCO) thick films grown by liquid phase epitaxy (LPE) as well as in top-seeded melt-textured growth (TSMTG) YBCO bulks prepared by cold seeding.[4,5] This phenomenon is attracting even more interest. Until now, many studies have dealt with the correlation between the intrinsic microstructure of YBCO thin films and the thermal stability. In this respect, the effects of the in-plane and out-of-plane orientation of YBCO grains and their volume ratio have been interpreted in terms of the YBCO surface energy and the YBCO/MgO boundary interface energy.[6−8] However, these cases were restricted to only air environment.

The present work addresses the thermal stability of YBCO thin films under an oxygen atmosphere. It is known that during YBCO bulk growth by means of TSMTG, the growth rate in an elevated oxygen pressure is higher than that in air, whereas the superconducting properties are not affected.[9] Therefore, oxygen pressure rise is an effective way to increase the growth rate of YBCO bulks. In this work, we present a detail comparison of the melting modes of YBCO thin films with various in-plane orientations, grown in oxygen. By means of a high-temperature optical microscope (HTOM), melting and growth of YBCO thin films were observed in situ. We found strong differences in the melting behavior of YBCO thin films with different in-plane orientations. A crucial effect of geometry and of the type of the terminal plane between the film and substrate on the melting behavior was observed.

Experimental Section

Two YBCO thin films were deposited by magnetron sputtering onto MgO (100) substrates 200 nm thick. The samples were deposited at 740 °C in Ar/O_2 mixture by means of the inverted cylindrical target sputtering with a biaxially rotating substrate. For the 45°-aligned films, an off-axis angle (<5°) substrate and an additional nitrogen gas were applied, which were derived by our experiments to be beneficial to the growth of the 45°-oriented films.

Both investigated films were *c*-axis-oriented, according to the pole figure test (D8 Discover GADDS, Bruker AXS) but had different in-plane orientations. The 0°- and 45°-aligned films were labeled A and B, respectively.

The melting behavior of the films was observed in situ by the optical microscope Olympus BX51 M with a high-

* Corresponding author. Tel: +86-21-54745772. Fax: +86-21-54745772. E-mail: xyao@sjtu.edu.cn.
[†] Ministry of Education.
[‡] Shanghai Jiao Tong University.
[§] Chinese Academy of Sciences.
[||] University of Electronic Science and Technology of China.
[⊥] Institute of Physics ASCR.

10.1021/jp911806r
Published on Web 05/14/2010

TABLE 1: Heating Procedure of the YBCO Thin Films During HTOM Observations

sample	heating rate (°C/min)	limit (°C)	holding time (min)
A	80	980	3
	5	1075	3
	80	500	0
B	80	980	3
	5	1095	3
	80	500	0

temperature heating stage (TS 1500). This method provided a direct visualization of the film nucleation and propagation during the growth process. The apparatus allowed a maximum temperature of 1500 °C, which was calibrated by standard pure silver shavings melting in air at 961 °C. During the experiment, the temperature of the samples was measured by a Pt/Rh thermocouple and controlled within ±1 °C of the target value by a microcomputer. First of all, the specimens were cut into the size of 2 × 2 mm^2 and set onto a sapphire holder placed at the bottom of the heating stage. The heating procedure used for both films consisted of several steps with different heating rates. The process is summarized in Table 1.

After the nominal temperature of 980 °C was reached, the heating rate was reduced, and the substrate temperature was carefully regulated to ensure that the displayed temperature was consistent with the real temperature of the film. All heating was conducted under an oxygen atmosphere. Then, the specimen was cooled at a high rate to room temperature and taken out of the heating stage. The surface morphology was checked by optical microscopy. To demonstrate the atomic configuration at the 45° YBCO/MgO interface, the HRTEM images of film B were taken with the JEOL-2010 electron microscope with the point-to-point resolution of 0.194 nm.

Results and Discussion

Before the HTOM experiment was performed, the in-plane orientation of both films was checked by means of XRD pole figure method with the (103) diffraction. As illustrated in Figure 1a, on film A, a typical four-fold symmetry revealed that the deposited film possessed 0°-orientated grains (YBCO<100>$_{film}$// MgO<100>$_{substrate}$). In contrast, the pole figure of film B, Figure 1b, illustrated a 45° four-fold symmetry (i.e., YBCO<110>$_{film}$// MgO<100>$_{substrate}$), being in a significant distinction to Figure 1a, and proved that 45°-oriented grains do exist. The pole figure analysis of the two kinds of films unambiguously indicated YBCO grains with two different in-plane orientations, 0 and 45°.

The series of micrographs from our real-time observations by means of HTOM are presented in Figure 2. The micrographs

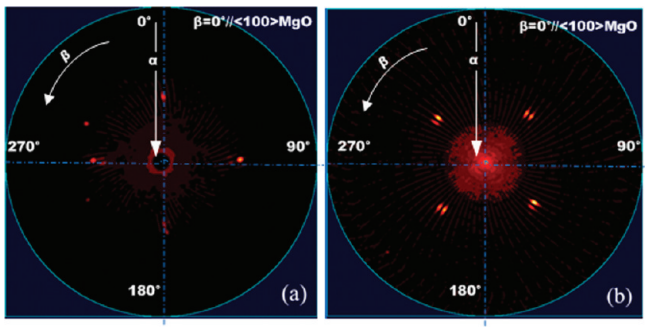

Figure 1. XRD pole figures of two YBCO thin films: (a) film A and (b) film B.

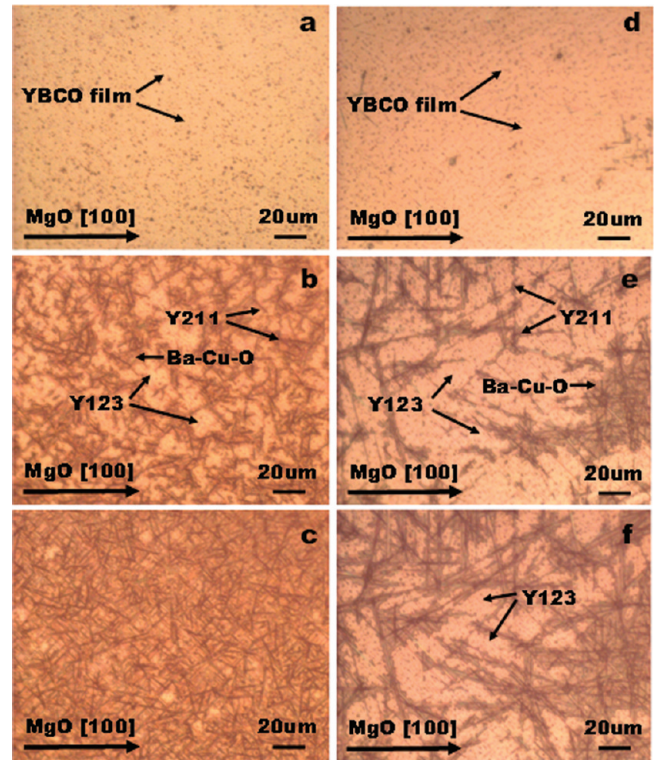

Figure 2. Optical micrographs showing the melting processes of films A and B, respectively: (a,d) in the initial melting stage of ~1009 °C; (b,e) at 1060 °C; (c,f) at 1070 °C.

of the two specimens, taken at the same temperatures, explicitly illustrate the differences in the melting processes of the two YBCO thin films.

As shown in Figure 2a, the morphology of the thin film A presented no change from room temperature to ~1009 °C, and no melting was observed. When temperature further rose, many small needle-like Y_2BaCuO_5 (Y-211) grains gradually appeared under the film surface, indicating that the Y-211 crystals can nucleate at some defect regions. Furthermore, Ba−Cu−O melt (decomposition product of YBCO) could be seen to cover the Y-211 crystals because of a high wettability of Y-211 by the Ba−Cu−O solvent. When temperature reached 1060 °C, the majority of the Y-123 film decomposed (Figure 2b), and small Y-211 crystals showed a tendency to surround the remaining YBCO area. The morphology of film A at 1070 °C, with the proceeding peritectic reaction, is shown in Figure 2c. Obviously, the Y-211 grains rapidly developed and quickly spread all over the surface.

Figure 2d−f shows the evolution of film B within the similar temperature range (1009−1070 °C). Figure 2d shows that a few acicular Y-211 crystals gradually grew from the undersurface of film B at 1009 °C. During the heating from 1009 to 1060 °C, Y-211 grains continued in nucleating and growing. (See Figure 2e.) Figure 2f shows a section of film B held at 1070 °C. The majority of the film exhibited the same morphology as that at the beginning, implying that an extensive melting behavior had not taken place yet. The YBCO grains of film B completely decomposed at 1095 °C. This means that a remarkable superheating exists in film B, and the thermal stability of film B is much better than that of film A.

After the growing process, the samples were taken from the heating stage, and their surface morphology was compared using optical microscopy (Figure 3). A dense structure of small Y-211 crystals can be observed in film A (Figure 3a). The Y-211

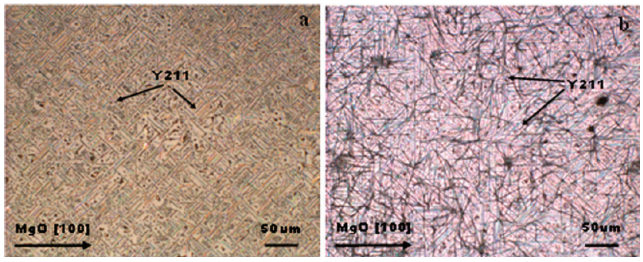

Figure 3. Comparison of the surface morphology of YBCO films after the melting process: (a) film A and (b) film B.

TABLE 2: Differences in the Melting Behaviors and Melting Modes of Films A and B Grown in Air and O_2 Atmosphere[a]

atmosphere	film	decomposition temperature T_{start} (°C)	decomposition temperature T_{end} (°C)	$T_{end} - T_{start}$ (K)
air	A(0°)	970	1060	90
	B(45°)	967	1020	53
O_2	A(0°)	1009	1070	61
	B(45°)	1007	1095	88

[a] Decomposition temperatures T_{start} and T_{end} indicate the temperatures at which the YBCO thin films start and finish decomposition, respectively.

crystals show preferential growth orientation (Y-211<001>// MgO<110>) denoted as 45° Y-211. In film B (Figure 3b), the size of the Y-211 crystallites is bigger than that in film A, and crystals with different orientations coexist. The orientations of the Y-211 crystallites with respect to the MgO substrate are Y-211<001>//MgO<110>, Y-211<001>//MgO<100> (denoted as 45°Y-211 or 0°Y-211, respectively), and others. The differences in the melting behavior of films A and B are listed in Table 2.

The melting modes of films A and B under O_2 atmosphere are similar to those in air, as described by Wang et al.[8] In addition, both films presented superheating in all cases. However, the decomposition temperature strongly depends on the oxygen content in the atmosphere. As shown in Table 2, T_{start} of both films A and B in pure O_2 is higher than that in air, indicating that the peritectic temperature of YBCO increases with the increase in oxygen partial pressure, as commonly reported.[10] In O_2, T_{end} of film B is higher than that of film A. This result is in contrary to the situation in air. It means that in O_2, the 45°-oriented grains have a higher thermal stability than the 0°-oriented grains, although their thermal stability is lower than that of the 0°-oriented grains in air.

Obviously, the differences in melting behaviors of films A and B can be attributed to their different thermal stability, which in turn is strongly correlated to both intrinsic and extrinsic conditions, namely, the structure and the melting/growing atmosphere, respectively. The most important distinction between the two films is the different in-plane orientation. The thermal stability of both YBCO films is fully extrinsically determined by oxygen pressure.

The large differences in the melting behaviors of the films grown in air and oxygen (Table 2) require a careful study of the thermal stability of the YBCO films with different in-plane orientations. First, the geometrical factor should be taken into account. It is known that the lattice constants of YBCO vary with the oxygen content. The calculated lattice mismatch of the $YBa_2Cu_3O_{7-\delta}$ grains (for different oxygen contents, δ) with the MgO substrate is listed in Table 3. The data indicate that an oxygen content change leads to only a small lattice mismatch

TABLE 3: Lattice Mismatch of $YBa_2Cu_3O_{7-\delta}$ with Various Oxygen Contents and the MgO Substrate for the 0 and 45° In-Plane Orientations[a]

δ	lattice constants (Å) (measured data)	$\langle 100\rangle_{Y123}//\langle 100\rangle_{MgO}$ (0°) 1YBCO unit on 1MgO unit (%) (calculated data)	$\langle 100\rangle_{Y123}//\langle 110\rangle_{MgO}$ (45°) 3YBCO units on 2MgO units (%) (calculated data)
0.07	$a = 3.8227$	−9.221	−3.710
	$b = 3.8872$	−7.689	−2.086
0.27	$a = 3.8275$	−9.107	−3.589
	$b = 3.8875$	−7.682	−2.078
0.40	$a = 3.8349$	−8.931	−3.403
	$b = 3.8851$	−7.739	−2.139
0.52	$a = 3.8415$	−8.775	−3.237
	$b = 3.8778$	−7.913	−2.322
0.62	$a = 3.8510$	−8.549	−2.997
	$b = 3.8700$	−8.098	−2.519
0.72	$a = 3.8621$	−8.285	−2.718
	$b = 3.8621$	−8.285	−2.718
0.91	$a = 3.86$	−8.335	−2.771
	$b = 3.86$	−8.335	−2.771

[a] To achieve the best match, we also varied the number of units in the calculation.

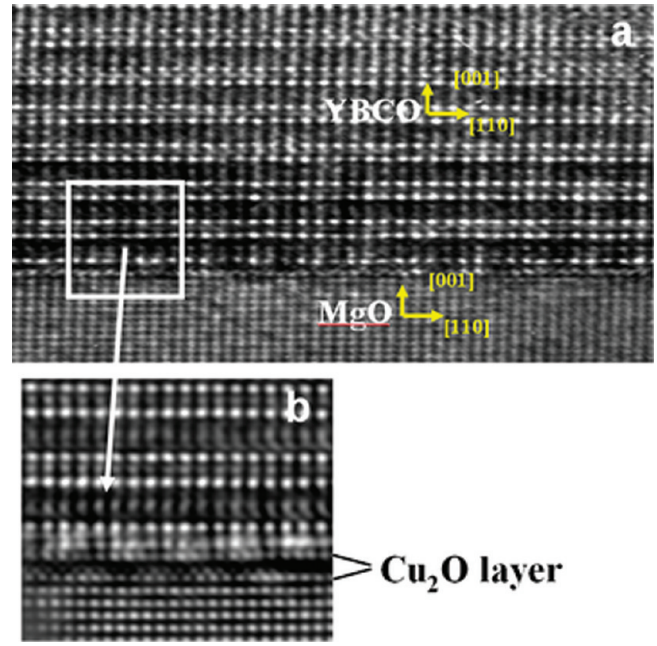

Figure 4. Cross-sectional HRTEM image of the 45°-oriented YBCO thin film on the MgO substrate. (a) General view of the interface between the 45°-oriented YBCO thin film and the MgO substrate. (b) Blow up of the square area on part a where the additional Cu_2O plane can be clearly seen.

change. It is evident that the variation of lattice constants caused by oxygen partial pressure has only a negligible effect on the lattice mismatch of the YBCO films and the MgO substrate.

Furthermore, the terminal plane of the film at the YBCO/MgO interface has to be taken into consideration because it considerably affects the Gibbs free energy. In the work of Matsuda et al.,[11] the HRTEM of a 0°-oriented YBCO film was investigated, showing that the grains were terminated by BaO layers. On the contrary, the atomic configuration of the 45°-oriented film B shows a big difference from that of film A (0°-oriented). Figure 4a is the HRTEM image of film B. The blow up part of the atomic configuration in vicinity of the interface, shown in Figure 4b, indicates that there are two unexpected rows of atoms between MgO and the BaO-CuO-BaO blocks of Y-123. These arrays have been deduced as a Cu_2O nanolayer

TABLE 4: Melting Behavior of the Cu_2O Powder in Air and Oxygen[a]

atmosphere	decomposition temperature T_{start} of the Cu_2O powder (°C)	decomposition temperature T_{end} of the Cu_2O powder (°C)	$T_{end} - T_{start}$ (K)
Air	1070	1076	6
O_2	1140	1149	9

[a] Decomposition temperatures T_{start} and T_{end} indicate the temperatures at which the Cu_2O powder starts and finishes decomposition, respectively.

based on the following two reasons: (1) Afrosimov et al. have demonstrated that Cu_2O possibly exists at the YBCO/MgO interface on the grounds of the middle-energy ion scattering study.[12] (2) The inserted atomic rows are shifted by ~0.21 nm along ⟨100⟩ MgO, which is consistent with the phenomena of Cu_2O (001) thin-film growth on MgO substrate.[13] It means that as an intermediate nanolayer, the Cu_2O phase exists between the 45°-oriented YBCO grains and the MgO substrate, which does not belong to the YBCO lattice. According to former experimental results[14,15] and the calculation of Granozio et al.,[16] the 0°-oriented YBCO grain with the BaO terminal layer (in air) has a more stable interface than the 45° grain with the Cu_2O intermediate layer. However, under the oxygen atmosphere in this work, the thermal stability of the 45°-oriented film B was considerably improved, getting even better than that of film A (0°-oriented). Therefore, we believe that the Cu_2O intermediate layer is responsible for the change in melting behavior and thermal stability of the film in oxygen atmosphere. From the chemical phase diagram, we see that the decomposition temperature of the oxide in a higher oxygen pressure is higher than that in lower oxygen pressure.[17] It is reasonable to deduce that the Cu_2O layer in film B has a higher decomposition temperature and a better thermal stability in pure oxygen than in air. This variation of thermal stability of the Cu_2O intermediate layer is most probably responsible for the different melting behaviors of the 45°-oriented films B grown in air and in oxygen.

We also investigated the thermal stability of Cu_2O under various atmospheres (air and oxygen). The structure of the Cu_2O layer between the YBCO and the MgO substrate was simulated by smearing Cu_2O powder on the MgO substrate surface. The Cu_2O powder was heated in the same manner as the YBCO thin film, and the melting behavior of the Cu_2O powder was observed in situ in a high-temperature optical microscope. The experimental results are listed in Table 4. The melting temperature of the Cu_2O powder in oxygen is much higher than that in air (by ~70 K for both T_{start} and T_{end}). This result is qualitatively consistent with the phase diagram analysis. The difference in melting temperatures of the film B and the simulated structure is due to the difference in the actual intrinsic structure (single layer and bulk). Therefore, it can be concluded that for film B, the reason of its higher thermal stability in oxygen is a good thermal stability of the Cu_2O terminal nanolayer. It suppresses the melting nucleation and shifts its occurrence to higher temperatures.

Previous works regarding the preferential growth mechanism of YBCO crystals on MgO substrates in the LPE growth process[18] showed that in pure oxygen, a polycrystalline YBCO seed film with an eight-fold symmetry transformed into a 45° LPE film; that is, that 45°-oriented seed grains survived and prevailed in the preferential growth, whereas the 0° seed grains decomposed during this process. This result indicated that in oxygen, the 45°-oriented YBCO seed grains had a more stable interface than the 0°-oriented grains, which is in good agreement with the present result that the thermal stability of film B (45°-oriented) is better than that of film A (0°-oriented). With the intermediate Cu_2O nanolayer, the YBCO thin films with different in-plane orientations display different thermal stability, which is of great importance for development of HTS devices and preparation of bulk REBCO materials with controlled specific properties. The most important point of this work is the universal conclusion that the thermal stability of a REBCO film can be significantly enhanced by inserting an intermediate buffer nanolayer. This fact is greatly beneficial for the REBCO film-seeded bulk growth, which always requires a seed material withstanding a higher processing temperature to suppress the homogeneous nucleation. We expect that the melting mechanisms and thermal stability of pure 0°- and 45°-oriented YBCO thin films elucidated in our work will be widely utilized in related experimental and theoretical works and will help to promote applications of 0°- and 45°-oriented YBCO thin films in electronics.

Conclusions

By means of the high-temperature optical microscopy, the melting behavior of YBCO/MgO thin films with different in-plane orientations was carefully observed under a pure oxygen environment. Our results clearly indicate that both 0°- and 45°-oriented films exhibit superheating properties, however, the thermal stability of the 45°-oriented films in oxygen is remarkably higher than that of the 0°-oriented films. It is in contrary to the experimental results for the same films melted in air. The effects of the oxygen partial pressure on the geometrical factor and the interface structure of the two YBCO thin film types have been clarified. The dramatic increase in thermal stability of the 45°-oriented film was explained by an intermediate Cu_2O nanolayer, which beneficially shifts the melting point upward with the rise of oxygen partial pressure.

Acknowledgment. We are grateful for the financial support from the NSFC (grant no. 50872082), the MOST of China (973 project no. 2006CB601003, 863 project no. 2007AA03Z206), Specialized Research Fund for the Doctoral Program of Higher Education, and Shanghai Science and Technology Committee of China (grant no. 08dj1400203). M.J. acknowledges the support from the grant of MEYS CZ no. ME 10069.

References and Notes

(1) Onnes, H. K. *Commun. Phys. Lab. Univ. Leiden* **1911**, *120b*, 122b.
(2) Bednorz, J. G.; Muller, K. A. *Z. Phys.* **1986**, *B64*, 189.
(3) Wu, M. K.; Asburn J., R.; Tony, C. J.; Hor, P. H.; Meng, R. L.; Gao, L.; Huang, Z. J.; Wang, Y. Q.; Chu, C. W. *Phys. Rev. Lett.* **1987**, *58*, 908.
(4) Yao, X.; Nomura, K.; Nakamura, Y.; Izumi, T.; Shiohara, Y. *J. Cryst. Growth.* **2002**, *234*, 611.
(5) Tang, C. Y.; Yao, X.; Hu, J.; Rao, Q. L.; Li, Y. R.; Tao, B. W. *Supercond. Sci. Technol.* **2005**, *18*, L31.
(6) Cai, Y. Q.; Yao, X. *Appl. Phys. A: Mater. Sci. Process.* **2005**, *81*, 1675.
(7) Tang, C. Y.; Cai, Y. Q.; Yao, X.; Rao, Q. L.; Tao, B. W.; Li, Y. R. *J. Phys: Condens. Matter.* **2007**, *19*, 076203.
(8) Wang, X.; Cai, Y. Q.; Yao, X.; Wan, W.; Li, F. H.; Xiong, J.; Tao, B. W. *J. Phys. D: Appl. Phys.* **2008**, *41*, 165405.
(9) Yan, S. B.; Chen, Y. Y.; Ikuta, H.; Yao, X. *IEEE Trans. Appl. Supercond.* **2010**, *20*, 66–70.
(10) Nakamura, M.; Krauns, C.; Shiohara, Y. *J. Mater. Res.* **1996**, *11*, 1076.
(11) Matsuda, J. S.; Oba, F.; Murata, T.; Yamamoto, T.; Ikuhara, Y.; Mizuno, M.; Nomura, K.; Izumi, T.; Shiohara, Y. *J. Mater. Res.* **2004**, *19*, 2674.

(12) Afrosimov, V. V.; Il'in, R. N.; Karmanenko, S. F.; Melkov, A. A.; Sakharov, V. I.; Serenkov, I. T. *Thin Solid Films* **2005**, *492*, 146.
(13) Takahiro, I.; Kunisuke, M. *Vacuum* **2007**, *81*, 904.
(14) Izumi, T.; Kakimoto, K.; Nomura, K.; Shiohara, Y. *J. Cryst. Growth.* **2000**, *219*, 228.
(15) Nomura, K.; Hoshi, S.; Yao, X.; Kakimoto, K.; Nakamura, Y.; Izumi, T.; Shiohara, Y. *J. Mater. Res.* **2001**, *16*, 979.
(16) Granozio, F. M.; di Uccio, U. S. *J. Alloys Compd.* **1997**, *251*, 56.
(17) Li, W. C. In *Metallurgy and Material Physical Chemistry*. Cao, S. L., Ed.; Metallurgical Industry: Beijing, China, 2001; Vol. 4, Chapter 3, pp 51−53.
(18) Cai, Y. Q.; Tang, C. Y.; Sun, L. J.; Yao, X.; Rao, Q. L.; Lai, Y. J. *J. Appl. Phys.* **2007**, *101*, 113907.

JP911806R